High-resolution scanning electron microscopy of atmospheric particles sampled at Jungfraujoch during the CLACE field experiment

Martin Ebert
Stephan Weinbruch

Technische Universität Darmstadt, Umweltmineralogie, Schnittspahnstr.9, D-64287 Darmstadt, Germany

Motivation

The optical properties of the atmosphere in the wavelength range of visible light are dominated by aerosol particles [1]. Aerosol particles can influence the atmospheric radiative balance by scattering and absorption (direct effects) and by acting as cloud condensation nuclei (indirect effects) [2]. For calculation of the scattering and absorption properties, detailed information about size, morphology, and chemical composition of the aerosol particles must be obtained [3-5].

Scanning electron microscopy combined with energy-dispersive X-ray microanalysis represents a powerful tool to determine these characteristic parameters. However, in the past two technical limitations have prevented the use of electron microscopy for the determination of the optical properties. First, the lateral resolution of conventional instruments is not sufficient for the study of morphological details of small particles (< 1 µm), which are important in order to assign particles into groups with defined optical properties. Second, conventional energy-dispersive detectors do often not allow the detection of the light elements carbon, nitrogen, and oxygen. Therefore, carbon-rich particles, the most important absorbing component of many atmospheric aerosols, could not be studied appropriately in the past.

By using a high-resolution instrument (field emission gun) equipped with a thin window X-ray detector these limitations were overcome and characterization of almost all components of the atmospheric aerosol is now possible. We have successfully applied this new technique to marine [6] and continental [7, 8] aerosols.

In the Lindenberg Aerosol Characterization Experiment (LACE 1998), we have determined the size resolved complex refractive index from the analysis of individual particles [8]. In order to trace the change of the optical properties during passage of the boundary layer by individual particle analysis, we are planning a measuring campaign at the Jungfraujoch station, for which the CLACE field experiment served as a feasibility study.

Sampling

Twelve aerosol samples were collected from 15 March to 19 March (Table 1).

sampling day	sampling time
15.03.2000	8.40-12.40
15.03.2000	13.05-15.05
15.03.2000	15.05-17.05
15.03.2000	17.20-23.30

16.03.2000	9.00-15.00
16.03.2000*	15.05-21.10
17.03.2000	9.15-13.15
18.03.2000	9.00-14.00
18.03.2000	14.00-19.30
19.03.2000	7.30-10.30
19.03.2000	10.30-13.30
19.03.2000	13.30-16.25

*interstitial aerosol

Table 1: Sampling days and sampling time.

Aerosol particles were sampled on conducting glassy carbon disks in a self-constructed two-stage cascade impactor [9]. With a flow rate of 2 l/min, the cutoff diameter of the prefractionator is 25µm and the cut off diameter of the impactor stage is 0.1 µm. In order to obtain an appropriate loading on the sample carrier, the sampling time was varied between 2 and 6 hours. Too long sampling times must be avoided because of the requirements of scanning electron microscopy, where overloading of the sample carrier may prevent an analysis of individual particles. The optimum sampling time depends on the total particle concentration and was estimated prior to sampling by means of an optical particle counter.

High-Resolution Scanning Electron Microscopy

Individual aerosol particles were studied by high-resolution scanning electron microscopy (HRSEM) and energy-dispersive X-ray microanalysis (EDX). For this purpose, the conducting glassy carbon disks were introduced directly into the instrument without carbon coating. The small grain sizes and the conductive substrate prevent the insulating phases from substantial charging during electron bombardment. All aerosol particles were studied with a field emission gun scanning electron microscope (PHILIPS XL 30 FEG). This instrument permits characterization of individual aerosol particles with diameters down to 10 nm, with excellent quality of the secondary electron (SE) images. X-ray analysis is carried out with an energy-dispersive Si(Li) detector (ultrathin window) allowing detection of elements with $Z \geq 5$ (boron). With this instrument size, morphology and elemental composition of individual aerosol particles can be determined. If the phase composition is needed for further interpretation of the data, transmission electron microscopy (TEM) has to be carried out.

With the applied method, we achieve a complete characterization (size, morphology, chemical composition and by use of TEM also phase composition) of the optically most important size range (100 nm - 3 µm; [10]) of atmospheric aerosols. With this information it is possible to derive the size-resolved complex refractive index from the analysis of individual aerosol particles. However, as the techniques used in the present study require high vacuum conditions during analysis, all the water present in the aerosol sample (except water enclosed in the crystal structure) is lost. The refractive index obtained from our approach is, thus, only feasible for relative humidities below the deliquescence point of the major aerosol components present.

Results and Discussion

As our participation in the CLACE field experiment is regarded as a feasibility study, we have analyzed only approximately 100 particles per sample. This number is adequate to determine the main particle groups with relative abundances ≥ 5 %. With the knowledge of the main particle groups some important properties of the aerosol, e.g., the deliquescence behavior and the average refractive index, can be estimated.

The particles were classified into ten different groups, using compositional and morphological criteria (Table 2).

particle group	criteria based on beam resistance and relative X-ray intensities [sum of net counts of elements with 11 ≤ Z ≤ 82 = 100 %]
silicium oxide (quartz)	Si > 85 %
alumosilicates	Si > 50 % and Al > 15 %
metal oxides/hydroxides	Fe > 80 %
calcium sulfate (gypsum)	Ca > 30 % and S > 40 %
ammonium sulfate	O + S > 80 %, beam damage

carbon rich particles	criteria based on morphology, beam resistance and relative X-ray intensities [sum of net counts of elements with 6 ≤ Z ≤ 82 = 100 %]
soot	morphology
biological	morphology and/or characteristic minor elements (Na, Mg, P, Cl, K and Ca)
C/silicate mixed particles	C + O + Al + Si > 80 %
C/SO_4 mixed particles	C + O + S > 80 % and Al + Si < 5 %, beam damage
C_{rest}	rest fraction of carbon dominated material, no beam damage

Table 2: Criteria for definition of particle groups.

During the whole time period from 15 to 19 March 2000, the three particle groups of soot, ammonium sulfates and alumosilicates were dominating. Soot and ammonium sulfates were often internally mixed.

According to our definition, all particles with variable composition between H_2SO_4 and $(NH_4)_2SO_4$, depending on the degree of neutralization of H_2SO_4 by NH_3, are assigned to ammonium sulfate. The original sulfate species and the water content are difficult to obtain by SEM investigations. When sulfate particles are deposited on the impactor stage, post-sampling alteration will occur during storage and SEM investigation. In Figure 1 typical ammonium sulate particles (dried droplets) are displayed. In Figure 2, a typical soot agglomerate is shown. Soot is defined here as an agglomeration of spherical particles

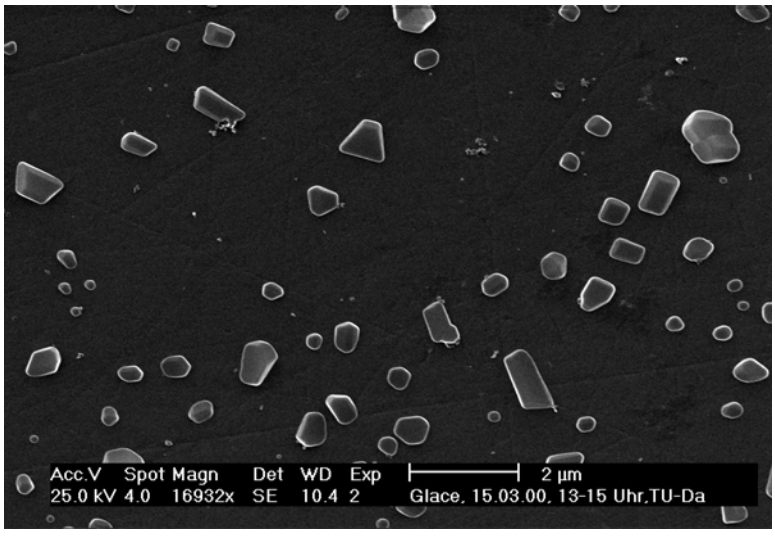

Figure 1: Secondary electron image of ammonium sulfate particles.

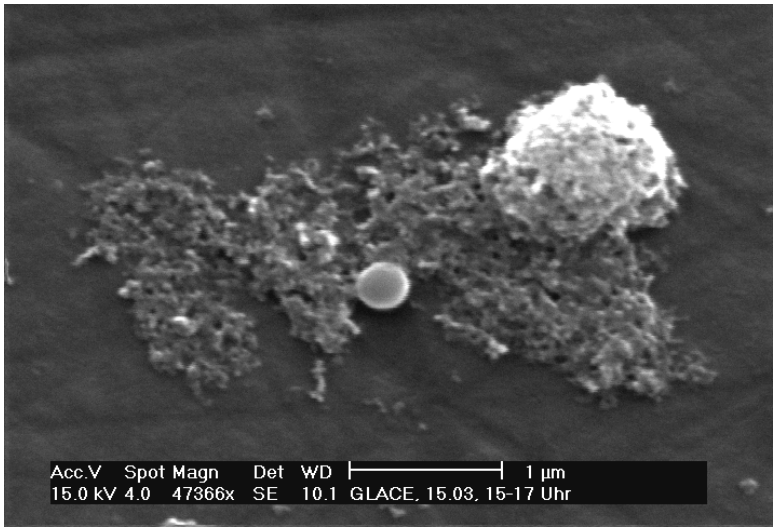

Figure 2: Secondary electron image of a typical soot agglomerate.

with diameters of the primary particles between 20 and 100 nm. In high-resolution scanning electron microscopy soot can be easily recognized in most cases by its characteristic morphology. Aged soot agglomerates may lose their characteristic primary texture and will, then, be assigned to the group of C_{rest}. The volume of the soot agglomerates is difficult to determine by electron microscopy due to their fractal geometry ([11-13]). Particle volumes in electron microscopy are usually calculated on the basis of the measured projected area diameters. However, this procedure leads to a systematic overestimation, as the pore volume of the soot agglomerates is not considered. The pore volume is highly variable depending on the size, source and history of the soot agglomerates. During the CLACE 98 field experiment, we have estimated that the average pore volume of ambient soot agglomerates will be in the range of 30 – 90 %, with the best estimate around 60 % [8]. Soot was not expected to be a main component of the aerosol at the Jungfraujoch station. It appears that the major part of the detected agglomerates is a contamination from fire activities in the Jungfraujoch train station. The absence of strong local particle sources is one of the most important requirements for aerosol sampling locations (and therefore under normal conditions a major advantage of the Jungfraujoch station). In Figure 3, typical alumosilicate particles are displayed. This particle group dominates the samples from 17, 18, and 19 March. According to air mass back-trajectories (Weingartner, pers. comm.), the silicates are desert dust and originate from a strong dust storm in Northwestern Africa. Many silicate particles contain some carbon, which may be explained by a second component, which is internally mixed with the silicates. We have, thus, defined the additional particle group of carbon/silicate mixed particles. At present, transmission electron microscopic investigations are carried out to identify the silicatic phases and to obtain more information about the carbon dominated material.

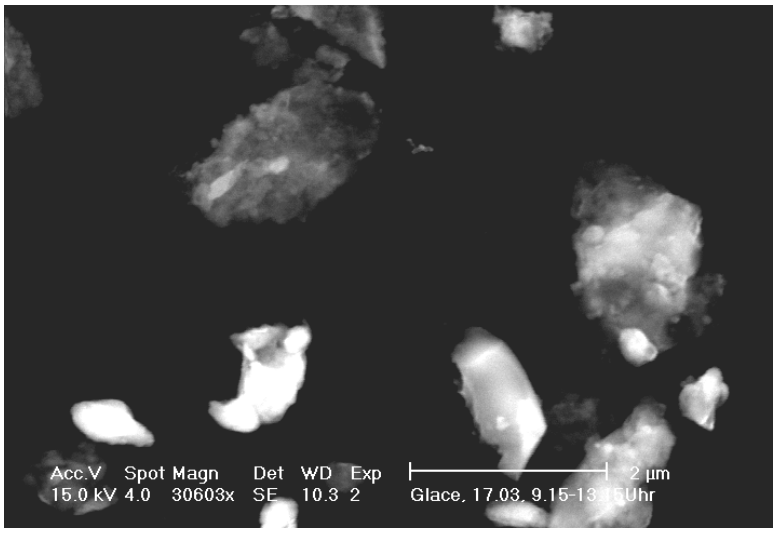

Figure 3: Secondary electron image of alumosilicate particles.

Besides the main particle groups outlined above, a few metal oxides/hydroxides particles, biological particles, calcium sulfates and C_{rest} particles have been observed. The results of our preliminary investigation are summarized in Table 3.

sample	**$D_{ae} \leq 1$ µm**			**$D_{ae} > 1$ µm**		
	dominant	*common*	*rare*	*dominant*	*common*	*rare*
03/15 8.40-12.40	soot	ammonium sulfate	-	soot	ammonium sulfate	-
03/15 13.05-15.05	C/SO_4	ammonium sulfate, soot	-	ammonium sulfate	-	-
03/15 15.05-17.05	soot		ammonium sulfate	soot	-	$CaSO_4$
03/15 17.20-23.30	soot	C_{rest}	-	-	silicates, soot, ammonium sulfate	-
03/16 09.00-15.00	-	soot, C/SO_4	-	soot	C/silicate	metal oxides
03/16 15.05-21.10	soot	metal oxides, silicates	-	soot	metal oxides, silicates	-
03/17 09.15-13.15	C/silicate	silicates	-	C/silicate	silicates	-
03/18 09.00-14.00	C/silicate	-	C_{rest}	C/silicate	-	C_{rest}, biological
03/18 14.00-19.30	C/silicate	soot, C_{rest}	-	C/silicate	C_{rest}	biological, C/$CaSO_4$
03/19 07.30-10.30	C/silicate	-		C/silicate	-	-
03/19 10.30-13.30	C/silicate	-	soot	C/silicate	-	soot
03/19 13.30-16.25	silicate	-	-	silicate	-	-

*interstitial aerosol

Table 3: Abundance of the different particle groups with diameters above and below 1 µm (dominant: > 50 %;0 common: 5 - 50 %; rare: < 5 %).

References

[1] Horvath, H., Spectral extinction coefficients of rural aerosol in southern Italy – a case study of cause and effect of variability of atmospheric aerosol, J. Aerosol Sci., **27**, 437-453 (1996).

[2] IPPC, Climate Change 1994, edited by Houghton et al., Cambridge Univ. Press, New York (1994).

[3] Tegen, I., P. Hollrig, M. Chin, I. Fung, D. Jacob, and J. Penner, Contribution of different aerosol species to the global aerosol extinction optical thickness: Estimates from model results, J. Geophys. Res., **102**, 23895-23915 (1997).

[4] Ten Brink, H.M., C. Kruisz, G.P.A. Kos, and A. Berner, Composition/size of the light-scattering aerosol in the Netherlands, Atmos. Environ., **31**, 3955-3962 (1997).

[5] Meszaros, E., A. Molnar, and J. Ogren, Scattering and absorption coefficients vs. chemical composition of fine atmospheric aerosol particles under regional conditions in Hungary, J. Aerosol Sci., **29**, 1171-1178 (1998).

[6] Ebert, M., S.Weinbruch, P. Hoffmann, and H.M. Ortner, Chemical characterization of North Sea aerosol particles, J. Aerosol Sci., **31**, 613-632 (2000).

[7] Weinbruch, S., M. Ebert, and P. Hoffmann P., Chemische Zusammensetzung und optische Eigenschaften von Aerosolpartikeln des Kleinen Feldbergs (Taunus)., Terra Nostra 2000/2, 121-122 (2000).

[8] Ebert, M., S. Weinbruch, A. Rausch, G. Gorzawski, G. Helas, P. Hoffmann, and H. Wex, The complex refractive index of aerosols during LACE 98 as derived from the analysis of individual particles, J. Geophys.Res., submitted.

[9] Weber, S., Bestimmung von Eisen und Identifizierung von Eisenverbindungen in partikulären Aerosolen, PhD thesis Technische Hochschule Darmstadt (1997).

[10] Seinfeld, J.H., and S.N. Pandis, Radiative effects of atmospheric aerosols: Visibility and climate in atmospheric chemistry and physics, John Wiley and Sons, New York (1998).

[11] Katrinak, K.A., P. Rez, P.R. Perkes, and P.R. Buseck, Fractal geometry of carbonaceous aggregates from an urban aerosol, Environ. Sci. Technol., **27**, 539-547 (1993).

[12] Skillas, G., S. Künzel, H. Burtscher, U. Baltensberger, and K. Siegmann, High fractal-like dimension of diesel soot agglomerates, J. Aerosol Sci., **29**, 411-419 (1998).

[13] Dye, A.L., M.M. Rhead, C.J. Trier, The quantitative morphology of roadside and background urban aerosol in Plymouth, UK, Atmos. Environ., **34**, 3139-3148 (2000).